RELATIVE-ERROR-BASED FINITE ELEMENT ANALYSIS OF AXIALLY MOVING BEAMS

Y.L. Kuo and W.L. Cleghorn
Department of Mechanical and Industrial Engineering, University of Toronto,
5 King's College Road, Toronto, Ontario, Canada M5S 3G8
Contact: ylkuo@mie.utoronto.ca

K. Behdinan
Department of Aerospace Engineering, Ryerson University,
350 Victoria Street, Toronto, Ontario, Canada M5B 2K3

Received April 2005, Accepted July 2006
No. 05-CSME-17, E.I.C. Accession 2869

ABSTRACT

The *r*-refinement increases accuracy of finite element solutions, but not increases computations. This paper presents a new and efficient technique applied to the *r*-refinement, which is based on the relative errors. This technique does not need a reference solution, and any physical quantity, such as energy, displacement, stress, etc., can be arbitrarily selected and applied to this technique. A simple algorithm is provided to find the optimum positions of nodes instead of solving a variety of nonlinear equations. Furthermore, this paper demonstrates this technique and provides a comprehensive finite element analysis of flexible axially moving beam by using the *h*-, *p*- and *r*-refinements.

"L'ERREUR RELATIVE A BASÉ" L'ANALYSE D'ÉLÉMENT FINIE DE DÉPLACER AXIALEMENT DES BIELLES

RÉSUMÉ

Le r-raffinement augmente l'exactitude de solutions d'élément finies, mais pas comptes d'augmentations. Ces présents de papier une technique nouvelle et efficace s'est appliquée au r-raffinement, qui est fondé sur les erreurs relatives. Cette technique n'a pas besoin d'une solution de référence et n'importe quelle quantité physique, comme l'énergie, le déplacement, la tension, etc., peut arbitrarily choisi et s'est appliquée à cette technique. Un algorithme simple est fourni pour trouver les positions optimales de noeuds au lieu de résoudre une variété d'équations non linéaires. En outre, ce papier démontre cette technique et fournit une analyse d'élément finie complète de bielle flexible axialement bougeante en utilisant le h-, p-et les r-raffinements.

1. INTRODUCTION

There are three common approaches used to increase the accuracy of finite element solutions. The h-refinement increases the number of elements. The p-refinement increases the degrees of interpolation functions. The r-refinement usually uses a coarse mesh, and the nodes are redistributed to increase accuracy. To compare the three refinements, the h- and p-refinements increase the level of accuracy by imposing more nodal variables. This causes more computations and larger data in programming codes. However, this r-refinement does not increase the computational cost while increasing accuracy. In 1978, Babuska and Rheinboldt [1] have addressed that the node distribution is asymptotically optimal if the selected error measure is distributed evenly, and that this optimum error is rather stable under perturbations of the node distribution. Hence, it is not necessary to locate more nodes with excessive accuracy. Furthermore, for some specific cases, an adequate mesh associated with the r-refinement can even produce a more accurate solution than an excessively fine mesh [2]. Thus, this refinement is worth to be further exploited.

The main issue of the r-refinement is the criterion of node redistribution. There are two principal approaches, equidistribution mesh and direct minimization [3]. The concept of equidisbribution mesh is to map a set of irregular distributed nodes in the physical domain to a regular grid point in the computational non-dimensional domain by using a monitor function. For its implementations, most of them emphasize solving one- and two-dimensional differential equations [4-7]. Some researches have analyzed elasto-static problems by using the boundary element method [8-10]. Lakshmanan *et al.* [11] have applied this technique on static thick cantilever beam problem and transient analysis of wave propagation. The derivation of this technique uses a monitor function instead of a real error measurement. Hence, the critical issue is to define an adequate monitor function. Also, it cannot guarantee to obtain an approximated solution with a global error.

Direct minimization is to directly minimize a measure of errors. Using variational principle, this technique leads to a set of global finite element equations and another set of nonlinear equations, which are used to determine the positions of nodes. This technique is called moving finite element. Miller *et al.* [12-13] originally presented this method in 1981. Baines [14] has presented a clear understanding of moving finite element method including relevant examples as well as some numerical results. This method has been widely used to solve partial differential equations [15-17]. Most of the works are based on the minimization of the residual of the partial differential equations [18-19]. Jimack [20] has applied moving finite element method on linear elasto-static problems and minimized the energy function by inserting an artificial time parameter in order to obtain an optimum mesh. This technique produces more unknown variables, and those nonlinear equations will become more complicated to be solved due to the velocities of node movement involved in dynamic problems.

Axially moving beams arise in diverse mechanical systems associated with spacecraft antennas, telescope robotic manipulators, and high-speed magnetic drives. A dynamic model of these systems with flexibility is needed for analysis and design. The traveling Euler-Bernoulli beams are the most common models of axially moving continua. Tabarrok *et al.* [21-23] derived the equations of motion consisting of continuity equations, momentum equations and mass-tension relations and solved them by the method of characteristics. Recently, flexible extendible beams have gained prominence due to new applications in the area of robotics. A modified Galerkin's method is used to solve the equation of motion of an axially moving beam [24]. The assumed-modes methods are used to compare the simulation results with those obtained experimentally [25]. Stylianou *et al.* [26-27] developed elements with time-varying domains to investigate the dynamics and stability analysis of the flexible extendible beam under more general configurations by the finite element method. Behdinan *et al.* [28-30] developed equations of motion for the geometrically nonlinear analysis of flexible sliding beams, deployed or retrieved through a rigid channel by using an extension of Hamilton's principle. Two approaches can be considered in the finite element method. One approach to deal with this class of problems is to employ beam elements of fixed lengths and to increase or decrease the number of elements as the motion of the beam varies. This approach is impossible to be implemented practically. The other approach is to use a fixed number of elements, but it is necessary to establish a beam element of variable space-domain beam.

This paper presents a simple technique to determine the positions of nodes while employing the *r*-refinement. A physical quantity, such as energy, displacement and stress, can be arbitrarily selected and inserted into this technique in order to obtain an optimum mesh, which has a minimum error associated with this quantity. A relevant mathematical algorithm is also provided, which can easily applied to any application problems. Furthermore, an axially moving beam is selected to demonstrate the efficiency of this technique. It is difficult to precisely predict the response of this beam due to its spatial domain changing with time. The Euler-Bernoulli beam theory is used to model this problem, and the results obtained by the *r*-refinement are also compared with those by the *h*- and *p*-refinements. To the best knowledge of the authors, this beam problem has not been solved either by either the *r*-refinement, or by the higher-degree beam elements like quintic polynomials. This paper will present a systematic study of this beam problem by these approaches.

2. RELATIVE-ERROR-BASED TECHNIQUE

The relative-error-based technique is developed in order to be applied in the *r*-refinement. This technique is based on a relative error, which is defined as the difference between two finite element solutions as follows [31]:

$$e_{ref}(\{X_1\},\{X_2\}) = \frac{\int_{t_1}^{t_2} [Q(t,\{X_1\}) - Q(t,\{X_2\})]^2 \, dt}{\|\{X_1\} - \{X_2\}\|} \tag{1}$$

where (t_1, t_2) is a time interval considered in application problems; vectors $\{X_1\}$ and $\{X_2\}$ are two sets of positions of internal nodes; Q is a time-dependent physical quantity of finite element solutions associated with a set of positions of the internal nodes. The quantity Q can be arbitrarily selected, such as displacement, stress, strain, energy, etc.

In this technique, an optimization problem is performed, which is to minimize a relative error in order to determine a set of positions of the internal nodes. When the norm of difference between vectors $\{X_1\}$ and $\{X_2\}$ approaches to zero, Equation (1) can be analogous to the differentiation of the quantity Q with respect to positions of the internal nodes. Hence, there is a minimum value associated with the quantity Q while the relative error is zero.

Based on the definition of the relative error, a mathematical algorithm for a two-element one-dimensional problem is listed in the following:

1) Set a non-dimensional initial position of the internal node, ${}^{(i)}x_N$ (the superscript (i) refers to ith iteration.)
2) Set the position step ${}^{(i)}\Delta x$, which is a distance from ${}^{(i)}x_N$. Then, two test points are expressed as ${}^{(i)}x_L = {}^{(i)}x_N - {}^{(i)}\Delta x$ (left test point) and ${}^{(i)}x_R = {}^{(i)}x_N + {}^{(i)}\Delta x$ (right test point).
3) Calculate the physical quantities, $Q(t, {}^{(i)}x_L)$, $Q(t, {}^{(i)}x_N)$ and $Q(t, {}^{(i)}x_R)$.
4) Calculate the relative errors, $e_{ref}({}^{(i)}x_N, {}^{(i)}x_L)$ and $e_{ref}({}^{(i)}x_N, {}^{(i)}x_R)$.
5) Compare the two relative errors:

(a) If $e_{ref}({}^{(i)}x_N, {}^{(i)}x_L) < e_{ref}({}^{(i)}x_N, {}^{(i)}x_R)$, then ${}^{(i+1)}x_N = {}^{(i)}x_L$ and ${}^{(i+1)}\Delta x = {}^{(i)}\Delta x$.

(b) If $e_{ref}({}^{(i)}x_N, {}^{(i)}x_L) > e_{ref}({}^{(i)}x_N, {}^{(i)}x_R)$, then ${}^{(i+1)}x_N = {}^{(i)}x_R$ and ${}^{(i+1)}\Delta x = {}^{(i)}\Delta x$.

(c) If $e_{ref}({}^{(i)}x_N, {}^{(i)}x_L) = e_{ref}({}^{(i)}x_N, {}^{(i)}x_R)$, then ${}^{(i+1)}x_N = {}^{(i)}x_N$, and ${}^{(i+1)}\Delta x = {}^{(i)}\Delta x \times c_N$ (c_N is a constant close to 1, but not equal to 1).

6) Check if the updated position oscillates between positions ${}^{(i)}x_N$ and ${}^{(i+1)}x_N$, while $i \geq 2$.

(a) If ${}^{(i+1)}x_N = {}^{(i-1)}x_N$, ${}^{(i+1)}x_N = ({}^{(i)}x_N + {}^{(i+1)}x_N)/2$, and ${}^{(i+1)}\Delta x = {}^{(i+1)}\Delta x / 2$.

(b) If ${}^{(i+1)}x_N \neq {}^{(i-1)}x_N$, position ${}^{(i+1)}x_N x_{i+1}$ and distance ${}^{(i+1)}\Delta x$ do not be changed.

7) Check if the desired tolerance is satisfied.

(a) If errors $e_{ref}({}^{(i)}x_N, {}^{(i)}x_L)$ and $e_{ref}({}^{(i)}x_N, {}^{(i)}x_R)$ are smaller than the desired tolerance, then the result converges and the iterative procedure can be stopped.

(b) If the result does not converge, go back to Step 3).

This mathematical algorithm is constructed based on a one-dimensional problem discretized as two elements. This technique can be easily expanded to those cases with multiple internal nodes and multiple dimensional problems. In order to examine the results obtained by applying this technique, a non-dimensional absolute error indicator is defined as follows:

$$e_n = \sqrt{\frac{\int_{t_1}^{t_2} ({}^{(FE)}Q - {}^{(REF)}Q)^2 \, dt}{\int_{t_1}^{t_2} {}^{(REF)}Q^2 \, dt}} \tag{2}$$

where the superscripts (*FE*) and (*REF*) represents finite element and reference solutions. Eq. (2) will be applied to the axially moving beam in order to verify the relative-errors-based technique.

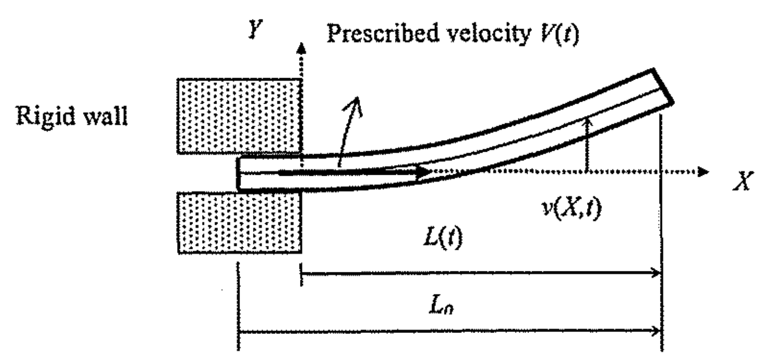

Figure 1: An axially moving beam

3. FINITE ELEMENT FORMULATION OF AXIALLY MOVING BEAMS

The beam is modeled based on the Euler-Bernoulli beam theory, and solved by using the finite element method. The difficulty of this problem is that the spatial domain is changing with time. The strategy of solving this problem is to discretize the beam as multiple elements, and the length of each element increases or decreases with time. Hence, the beam elements are constructed by utilizing the Liebnitz's rule.

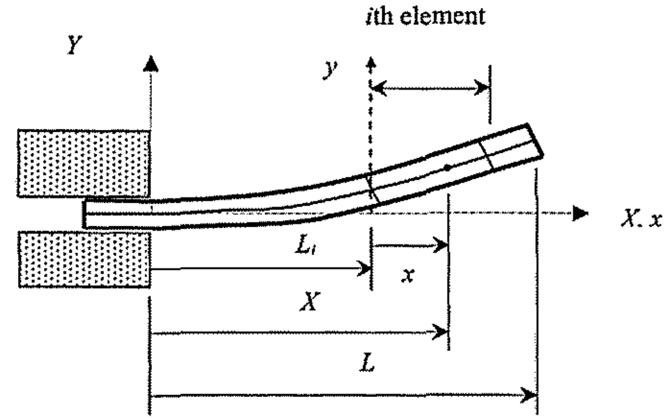

Figure 2: A beam element coordinate system

Fig. 1 shows an uniform beam of length $L(t)$ outside the rigid wall at time t, vibrating in the inertial coordinate system X-Y, and moving axially at a specified velocity $V(t)$ along the X-direction. The part of the beam inside the rigid wall is assumed as non-deformable and has a prescribed longitudinal motion. The length of this part is expressed as L_0-$L(t)$, where L_0 is the total length of the beam. Any arbitrary material point along the neutral axis of the beam is located by coordinate X, and the elastic transverse displacement of the point with reference to the neutral axis at time t by $v(X,t)$. There are three assumptions in this problem: the transverse displacement gradient v_x is small so that its second-degree term $(v_X)^2$ can be neglected; the beam is rigid or inextensible along its neutral axis, and hence the axial velocity $V(t)$ is independent of X; the acceleration field is time-dependent only. Then, the Lagranigan of this mechanical system may be given as [22]

$$L_g = \int_0^{L(t)} [\frac{1}{2}\rho A(\frac{\partial v}{\partial t} + V\frac{\partial v}{\partial X})^2 - \frac{1}{2}EI(\frac{\partial^2 v}{\partial X^2})^2]dX + \frac{1}{2}\rho A L_0 V^2 \tag{3}$$

where the three terms of the Lagrangian are the kinetic energy, the potential energy, and the longitudinal kinetic energy (a prescribed quantity), respectively.

In order to develop the finite element equations for the variable spatial domain beam element, a beam element coordinate system x- y is introduced and shown in Fig. 2. The longitudinal position of an arbitrary point on the beam element is expressed as x and X with respect to the inertial and the beam element coordinate systems, respectively. Quantity L_i is the position of the left-hand end of the beam element with respect to the inertial coordinate system. Then, the longitudinal velocity of an arbitrary point on the beam coordinate system is given as

$$\dot{x} = \dot{X} - \dot{L}_i \tag{4}$$

Since the beam has a rigid longitudinal motion, i.e., $\dot{X} = \dot{L} = V$ and $\dot{L}_i = (L_i / L)\dot{L}$, Eq. (4) is expressed as

$$\dot{x} = (1 - L_i / L)\dot{L} \tag{5}$$

Based on Eqs. (3) and (5), the Lagrangian of a beam element is

$$L_e = \int_0^{l(t)} \{\frac{1}{2}\rho A[v_t + (1 - \frac{L_i}{L})\dot{L}v_x]^2 - \frac{1}{2}EIv_{xx}^2\}dx + \frac{1}{2}\rho A l \dot{L}^2 \tag{6}$$

where l is the length of a beam element, which is also a function of time.

In the finite element method, an approximated transverse displacement can be expressed as

$$v = [N]\{\phi_e\} \tag{7}$$

where $[N]$ is a row vector in terms of shape functions, and $\{\phi_e\}$ is a column vector in terms of nodal values.

Performing the appropriate differentiations of the transverse displacement, it leads to

$$\dot{v} = [\dot{N}]\{\phi_e\} + [N]\{\dot{\phi}_e\} \tag{8}$$

Since matrix $[N]$ are functions of the coordinate x and the length of the beam $l(t)$, then

$$[\dot{N}] = \frac{d[N]}{dt} = \frac{\partial[N]}{\partial l}\frac{dl}{dt} \tag{9}$$

Applying the Euler-Lagrange equation and employing Eqs. (6) to (9), the element governing equation can be expressed as

$$[M_e]\{\ddot{\phi}_e\} + [C_e]\{\dot{\phi}_e\} + [K_e]\{\phi_e\} = \{F_e\} \tag{10}$$

where $[M_e]$, $[C_e]$ and $[K_e]$ are mass, equivalent damping and equivalent stiffness matrices of elements, $\{F_e\}$ is a load vector of elements, and $\{\phi_e\}$ is a vector of element variables. The mass matrix is symmetric, but the equivalent damping and stiffness matrices are in general not symmetric. The equivalent damping matrix depends on the mass matrix, i.e., if the mass is increasing, the equivalent damping matrix is positive definite, whereas if the mass is decreasing, it becomes negative definite. Since the free vibration of this system is considered, there are no applied forces, and the load vector is zero.

The global system equations are obtained by assembling the element equations and can be expressed as

$$[M]\{\ddot{\phi}\} + [C]\{\dot{\phi}\} + [K]\{\phi\} = \{F\} \tag{11}$$

where $[M]$, $[C]$, $[K]$ are global mass, equivalent damping and stiffness matrices, $\{F\}$ is a global load vector, which is also a zero vector, and $\{\phi\}$ is a vector of global variables. Eq. (11) is a set of linear second-order differential equations with variable coefficients. Based on the formulation, the axially moving beam problems are clearly non-conservative.

To account for the damping effects, a physical proportional damping matrix, is expressed as

$$[C_p] = \alpha [M] + \beta [K] \tag{12}$$

where α and β are two constants, which can be calculated by using the two experimental modal damping functions.

Table 1: Optimum non-dimensional positions of internal nodes

Test case	Number of elements	Uniform/ Adaptive mesh	Non-dimensional positions of internal nodes based on				
			Absolute/ Relative error indicator	Total energy	Tip displacement	Tip rotation	Clamped-end stress
1	2	Uniform	Absolute	0.5 (e=1.403E-3)	0.5 (e=1.136E-2)	0.5 (e=1.109E-2)	0.5 (e=1.506E-2)
		Adaptive	Absolute	0.5419 (e=1.290E-3)	0.6285 (e=5.857E-3)	0.5829 (e=7.704E-3)	0.5063 (e=1.503E-2)
			Relative	0.5420 (e=1.290E-3)	0.6281 (e=5.858E-3)	0.5827 (e=7.705E-3)	0.5072 (e=1.504E-2)
	3	Uniform	Absolute	0.3333, 0.6667 (e=2.817E-4)	0.3333, 0.6667 (e=2.409E-3)	0.3333, 0.6667 (e=2.429E-3)	0.3333, 0.6667 (e=4.460E-3)
		Adaptive	Absolute	0.3882, 0.6993 (e=2.469E-4)	0.4779, 0.7654 (e=1.116E-3)	0.4328, 0.7399 (e=1.510E-3)	0.2936, 0.6592 (e=4.188E-3)
			Relative	0.3879, 0.6988 (e=2.470E-4)	0.4725, 0.7619 (e=1.119E-3)	0.4367, 0.7341 (e=1.517E-3)	0.3104, 0.6602 (e=4.195E-3)
2	2	Uniform	Absolute	0.5 (e=2.619E-4)	0.5 (e=1.176E-2)	0.5 (e=8.73E-3)	0.5 (e=1.479E-2)
		Adaptive	Absolute	0.5441 (e=2.067E-4)	0.6294 (e=6.343E-3)	0.5938 (e=5.753E-3)	0.4577 (e=1.406E-2)
			Relative	0.5460 (e=2.077E-3)	0.6311 (e=6.354E-3)	0.5950 (e=5.764E-3)	0.4654 (e=1.420E-2)
	3	Uniform	Absolute	0.3333, 0.6667 (e=4.888E-5)	0.3333, 0.6667 (e=2.624E-3)	0.3333, 0.6667 (e=1.948E-3)	0.3333, 0.6667 (e=5.287E-3)
		Adaptive	Absolute	0.3910, 0.7012 (e=4.298E-5)	0.4770, 0.7634 (e=1.375E-3)	0.4417, 0.7460 (e=1.180E-3)	0.2216, 0.6213 (e=3.820E-3)
			Relative	0.3923, 0.7025 (e=4.231E-4)	0.4811, 0.7718 (e=1.391E-3)	0.4524, 0.7558 (e=1.196E-3)	0.2354, 0.6365 (e=3.964E-3)

e: Absolute Error

4. PRESCRIBED MOTIONS AND ERROR INDICATORS

In order to demonstrate the time responses of the beam by the finite element method, two kinds of motion profiles of the length of the beam are given as

Test case 1:

$$L(t) = L(0) + a_1 t + a_2 t^2 / 2 \tag{13}$$

where $L(0) = 0.4255$ (m), $a_1 = 0.0410$ (m/s), and $a_2 = 0$

Test case 2:

$$L(t) = L(0) + (c/\tau)[t - (\tau/2\pi)\sin(2\pi t/\tau)] \quad (14)$$

where $L(0) = 0.3500$ (m), $c = 0.7000$ (m), and $\tau = 1.200$ (sec)

Eq. (13) is a quadratic function of time, and it can provide the motion of the beam with constant velocity or acceleration. Basically, Eq. (14) a sinusoidal function of time, which is generated in order to reduce the vibration of the beam [24]. The beam has an extrusion motion based on two test cases.

The finite element analysis of this beam problem is demonstrated by using the *h*-, *p*- and *r*-refinements of the finite element method based on four error indicators. The selected physical quantity Q given in Eqs. (1) and (2) is total energy, the tip displacement, the tip rotation, and the clamped-end stress. The finite element model is solved by using the Newmark direct integration method with constant time-step size to obtain the transient response of the system. The reference solution of this beam problem is based on a two-node ten-element mesh with quintic shape functions. The time responses of the tip displacement of the beam for two test cases are shown in Figs. 3 and 4. The results obtained are in good agreement with Reference [24].

Table 2: Errors for test case 1 by the h-refinement with cubic shape functions

Number of element	Degrees of freedom	Non-dimensional errors based on			
		Total energy	Tip displacement	Tip rotation	Clamped-end stress
1	2	2.460E-2	1.111E-1	1.077E-1	1.342E-1
2	4	1.403E-3	1.136E-2	1.109E-2	1.506E-2
3	6	2.817E-4	2.409E-3	2.429E-3	4.460E-3
4	8	9.181E-5	7.856E-4	7.996E-4	2.086E-3

Table 3: Errors for test case 2 by the h-refinement with cubic shape functions

Number of element	Degrees of freedom	Non-dimensional errors based on			
		Total energy	Tip displacement	Tip rotation	Clamped-end stress
1	2	3.850E-3	1.122E-1	8.375E-2	1.139E-1
2	4	2.619E-4	1.176E-2	8.173E-3	1.479E-2
3	6	4.888E-5	2.624E-3	1.948E-3	5.287E-3
4	8	1.860E-5	9.081E-4	6.642E-4	2.849E-3

5. OPTIMUM MESHES BY THE RELATIVE-ERROR-BASED TECHNIQUE

This section presents the implementation of the *r*-refinement by using two- and three-element meshes. The goal is to find the optimum mesh by minimizing certain error indicators. The number of iteration for all test cases is below 50, and the tolerance set is the algorithm is 10E-4. Table 1 shows the non-dimensional optimum positions of the internal nodes based on the errors of total energy, the tip displacement, the tip rotation, and the clamped-end stress for two test cases [32]. The non-dimensional positions of internal nodes are defined as zero to one, based on the length of beam from the fixed end to the free end. This table also includes the absolute as well as relative error indicators, which are compared with the errors obtained by employing a uniform mesh. By applying the mathematical algorithm of the relative-error-based technique, the optimum mesh can be obtained. The results show that this algorithm can find the optimum positions of internal nodes, whose differences between those based on the absolute and the relative errors are below 0.01. To compare with the uniform meshes, the optimum positions of the internal nodes obtained for all test cases are slightly close to the free end. In other words, the uniform meshes cannot provide minimum errors in this beam problem. Especially for the tip displacement, the errors have almost a half of reduction.

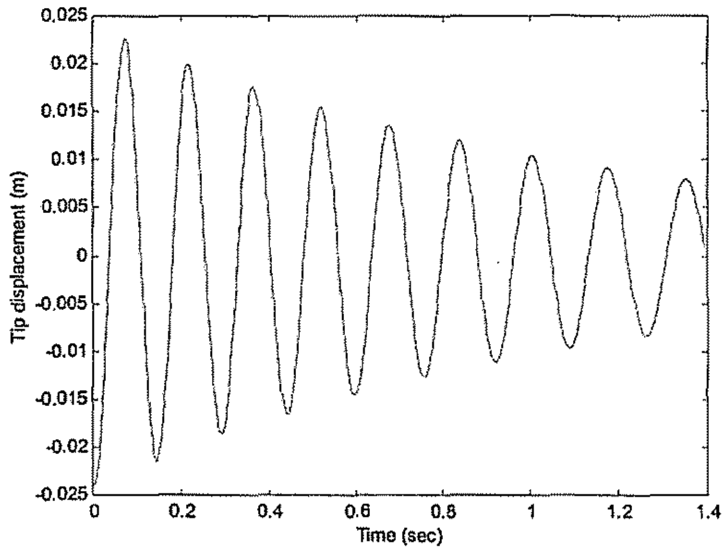

Figure 3: Time response of tip displacement for test case 1

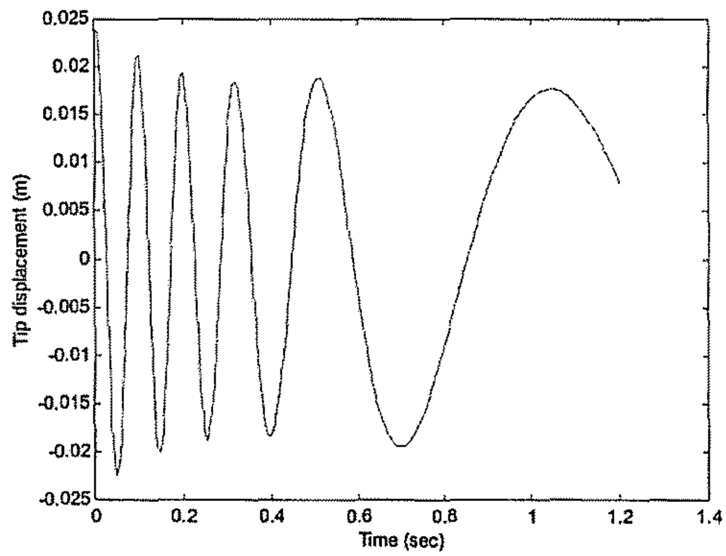

Figure 4: Time response of tip displacement for test case 2

6. ERROR ANALYSIS BY THE *H*- AND *P*-REFINEMENTS

This section presents the error analysis by the *h*-refinement of employing the beam element with cubic and quintic shape functions separately, and by the *p*-refinement.

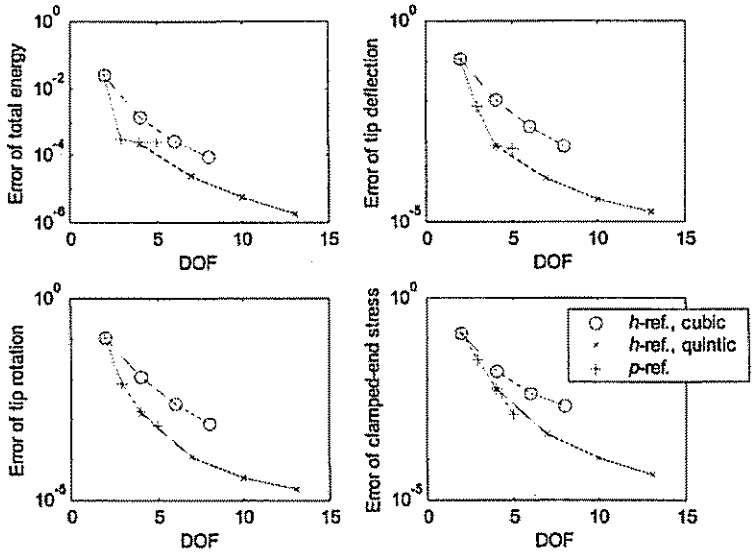

Figure 5: Errors by the h- and p-refinements for test case 1

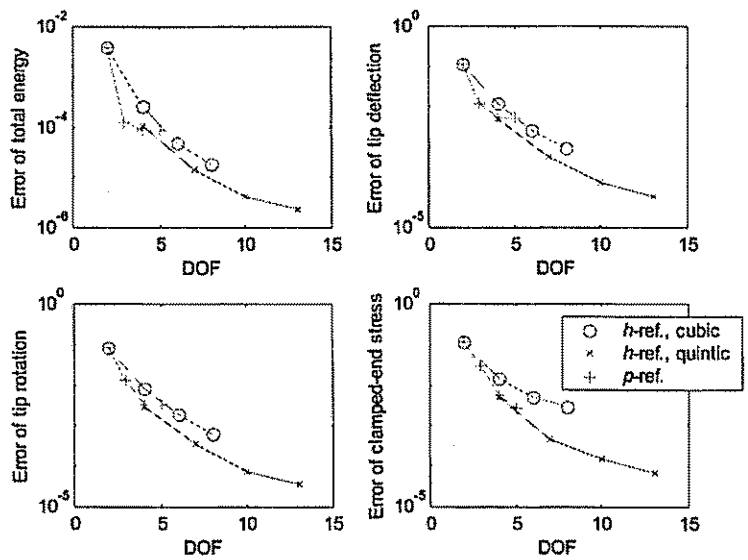

Figure 6: Errors by the h- and p-refinements for test case 2

6.1 The *h*-refinement based on the beam element with cubic shape functions

The beam element is based on two-node beam elements with cubic shape functions, and the beam is modeled by one, two, three and four equal-length elements. Tables 2 and 3 list the errors of the total energy, the tip displacement, the tip rotation, and the clamped-end stress. While requiring errors to be less than 1%, based on the errors of total energy, the suggested numbers of elements are two for test case 1 and one for test case 2. Based on the errors of tip displacement, the suggested numbers of elements are three for both test cases. Based on the errors of tip rotation, the suggested numbers of elements are three for test case 1 and two for test case 2. Based on the errors of clamped-end stress, the suggested number of element is three both all test cases. Comparing the two input motion profiles, the motion profile of the sinusoidal function produces smaller errors of total energy than the quadratic one under one- and two-element meshes.

6.2 The *h*-refinement based on the beam element with cubic shape functions

While implementing cubic shape functions, the bending stress and strain have linear relationship with the axial coordinate, and it is discontinuous at the inter-element nodes. This is inadequate to capture a required degree of accuracy. The two-node beam element based on quintic shape functions is employed in the *h*-refinement. Tables 4 and 5 list the errors of the total energy, the tip displacement, the tip rotation, and the clamped-end stress. For those cases of applying three or four elements with cubic shape functions, the errors are close to those of employing three or four elements with quintic shape functions. While requiring errors to be less than 1%, a one-element mesh is sufficient for both test cases based on all error indicators.

Table 4: Errors for test case 1 by the h-refinement with quintic shape functions

Number of element	Degrees of freedom	Non-dimensional errors based on			
		Total energy	Tip displacement	Tip rotation	Clamped-end stress
1	4	2.214E-4	7.520E-4	1.467E-3	5.717E-3
2	7	2.500E-5	1.243E-4	1.234E-4	4.229E-4
3	10	5.878E-6	3.585E-5	3.618E-5	1.088E-4
4	13	1.819E-6	1.790E-5	1.853E-5	4.343E-5

Table 5: Errors for test case 2 by the h-refinement with quintic shape functions

Number of element	Degrees of freedom	Non-dimensional errors based on			
		Total energy	Tip displacement	Tip rotation	Clamped-end stress
1	4	1.045E-4	4.922E-3	2.983E-3	5.280E-3
2	7	1.408E-5	5.565E-4	3.602E-4	4.796E-4
3	10	4.244E-6	1.295E-4	7.341E-4	1.480E-4
4	13	2.254E-6	6.072E-4	3.714E-4	6.837E-5

6.3 The *p*-refinement

This section presents the error analysis by considering one element on the beam and increasing the value of p, which is the highest degree of interpolation function. Tables 6 and 7 show the errors of the total energy, the tip displacement, the tip rotation, and the clamped-end stress. The results show that there are large error reductions between the values of p set as three and four. While requiring the errors to be less than 1%, the suggested degree of shape functions is four based on the total energy, the tip displacement, and the tip rotation for both test cases. Based on the clamped-end stress, the suggested degree of shape function is five for both test cases.

7. COMPARISONS OF THE *H*-, *P*- AND *R*-REFINEMENTS

First of all, the comparisons of employing the *h*-refinement based on cubic and quintic shape functions are presented. In most cases, employing quintic shape functions may produce smaller errors than employing cubic ones under the same number of degrees of freedom. It illustrates that higher-degree shape functions are more efficient.

Table 6: Errors for test case 1 by the p-refinement

Degrees of shape functions	Degrees of freedom	Non-dimensional errors based on			
		Total energy	Tip displacement	Tip rotation	Clamped-end stress
3	2	2.460E-2	1.111E-1	1.077E-1	1.342E-1
4	3	2.929E-4	7.655E-3	7.663E-3	3.044E-2
5	4	2.443E-4	8.038E-4	1.510E-3	5.709E-3
6	5	2.441E-4	6.800E-4	6.781E-4	1.332E-3

Table 7: Errors for test case 2 by the p-refinement

Degrees of shape functions	Degrees of freedom	Non-dimensional errors based on			
		Total energy	Tip displacement	Tip rotation	Clamped-end stress
3	2	3.850E-3	1.122E-1	8.375E-2	1.139E-1
4	3	1.247E-4	1.167E-2	1.313E-2	3.039E-2
5	4	8.266E-5	5.284E-3	3.332E-3	5.596E-3
6	5	8.260E-5	5.282E-3	3.322E-3	2.769E-3

Secondly, comparing the h- and p-refinements, Figs. 5 and 6 show the errors of total energy, tip displacement, tip rotation and clamped-end stress for both test cases. Since the h-refinement with quintic shape functions has more degrees of freedom, the errors are much smaller than other refinement methods. The p-refinement has a higher rate of convergence than the h-refinement while employing cubic shape functions. In general, higher degrees of freedom produce higher accuracies. However, the computational cost also increases. Table 8 shows the CPU time comparisons of the h- and p-refinements. The data are computed with a personal computer of INTEL Pentium II Processor 300 MHz. The programming language is MATLAB. The time step is 0.001 sec. The results show that the CPU time has a linear relationship with the number of degrees of freedom.

Since the implementation of quintic shape functions produces highly accurate approximated solutions, the r-refinement employs cubic shape functions by separately applying two and three elements in order to obtain the optimum positions of the internal nodes. While the positions of the internal node are either at the midpoint for two-element mesh or at one-third and two-thirds of the beam, these cases are the same with those of employing two and three elements with cubic shape functions, respectively. The errors obtained from employing the r-refinement are smaller than those from the h-refinement with cubic shape functions under the same number of elements. It illustrates that the equal-length mesh is not optimum, and the optimum positions of the internal nodes are highly dependent on the input motion profiles.

Table 8: CPU time comparison for the h- and p-refinements

Refinement methods	Number of elements			
	1	2	3	4
The h-refinement based on cubic shape functions	65.78 (sec.) (DOF = 2)	127.41 (sec.) (DOF = 4)	183.07 (sec.) (DOF = 6)	245.43 (sec.) (DOF = 8)
The h-refinement based on quintic shape functions	104.64 (sec.) (DOF = 4)	204.49 (sec.) (DOF = 7)	298.10 (sec.) (DOF = 10)	404.52 (sec.) (DOF = 13)

Refinement methods	Degree of shape functions			
	3	4	5	6
The p-refinement	99.82 (sec.) (DOF = 3)	132.05 (sec.) (DOF = 4)	168.76 (sec.) (DOF = 5)	217.73 (sec.) (DOF = 6)

DOF: Number of degrees of freedom

8. CONCLUSION

This paper presents a new technique applied to the *r*-refinement. To compare it with the existing techniques, there are several advantages: a physical quantity, such as energy, displacement, stress, etc., can be arbitrarily selected and inserted into this technique; a simple algorithm is provided instead of solving nonlinear equations; there is no need to have a reference solution; the number of equations solved does not increase; this technique can be applied to any application problems.

In order to demonstrate the efficiency of this technique, this paper also provides a comprehensive study of flexible axially moving beam about selecting refinements and error indicators. By applying the *h*- and *p*-refinements, the accuracy of finite element solutions increases as the number of degrees of freedom increases, no matter which error indicator is selected. However, the computational cost is also increased. By applying the *r*-refinement, the mesh of equal-length elements does not produce minimum errors, and the errors can be reduced to a half based on some error indicator. It illustrates that the *r*-refinement may have much improvement of error reduction, but computations and data space in computer codes do not increase.

REFERENCES

[1] Babuska, I. and Rheinboldt, W.C., "A-posteriori error estimates for the finite element method", *Int. J. Num. Meth. Eng*, 12, 1597-1615., 1978.

[2] Lang, J., Cao, W., Huang, W., and Russell, R.D., "A two-dimensional moving finite element method with local refinement based on a posteriori error estimates", *Appl. Num. Math*, 46, 75-94, 2003.

[3] Baines, M.J., "Grid adaptation via node movement", *Appl. Num. Math*, 26, 77-96, 1998.

[4] Eiseman, P.R. (1987), "Adaptive grid generation", *Comp. Meth. Appl. Mech. Eng.*, 64, 321-376.

[5] Kittur, M.G., Huston, R.L., and Oswald, F.B., "Finite element grid improvement by minimization of stiffness matrix trace", *Comp. Struct.*, 31, 891-896, 1989.

[6] Pereyra, V. and Sewell, E.G., "Mesh selection for discrete solutions of boundary-value problems in ordinary differential equations", *Num. Math.*, 23, 261-268, 1975.

[7] Chen, T.F. and Yang, H.D., "Numerical construction optimal adaptive grids in two spatial dimensions", *Comp. Math. Appl.*, 39(12), 101-120, 2000.

[8] Sun, W. and Zamani, N.G., "Adaptive mesh redistribution for the boundary element in elastostatics", *Comp. Struct.*, 36(6), 1081-1088, 1990.

[9] Sun, W. and Zamani, N.G., "An adaptive *h-r* boundary element algorithm for the Laplace equation", *Int. J. Num. Meth. Eng.*, 33, 537-552, 1990.

[10] Sun, W., "Two-dimensional mesh redistribution and solution of singular boundary value problems", *Commu. Num. Meth. Eng.*, 14, 797-808, 1998.

[11] Lakshmanan, S., Soni, B.K., and Balasubramaniam, K., "*r*-adaptation in finite element modeling of elastic solids", *Compu. Struct.*, 63(2), 249-257, 1997.

[12] Miller, K., "Moving finite elements, Part I", *SIAM J. Num. Anal.*, 18, 1019-1032, 1981.

[13] Miller, K. and Miller, R.N., "Moving finite elements, Part II", *SIAM J. Num. Anal.*, 18, 1033-1057, 1981.

[14] Baines, M.J., *Moving Finite Elements*, Oxford University Press, Oxford, 1994.

[15] Coimbra, M., Sereno, C., and Rodrigues, A., "Applications of a moving finite element method", *Chem. Eng. J.*, 84(1), 23-29, 2001.

[16] Coimbra, M., Sereno, C., and Rodrigues, A., "A moving finite element method for the solution of two-dimensional time-dependent models", *Appl. Num. Math.*, 44(4), 449-469, 2003.

[17] Baines, M.J., "Grid adaptation via node movement", *Appl. Num. Math.*, 26, 77-96, 1998.

[18] Zegeling, P.A. and Blom, J.G., "A note on the grid movement induced by MFE", *Int. J. for Num. Meth. Eng.*, 35(3), 623-636, 1992.

[19] Baines, M.J., "Analysis of the moving finite-element procedure", *SIAM J. Num. Anal.*, 28(5), 1323-1349, 1991.

[20] Jimack, P. K., "An optimal finite element mesh for elastostatic structural analysis problems", *Comp. Struct.*, 64(1-4), 197-208, 1997.

[21] Kim, Y.I. and Tabarrok, B., "On the nonlinear vibration of traveling strings", *J. Fran. Inst.*, 293(6), 381-399, 1972.

[22] Tabarrok, B., Leech, C.M., and Kim, Y.I., "On the dynamics of an axially moving beam", *J. Fran. Inst.*, 297(3), 201-220, 1974.

[23] Elmaraghy, R. and Tabarrok, B., "On the dynamic stability of an axially oscillating beam", *J. Fran. Inst.*, 300(1), 25-39, 1975.

[24] Wang, P.K.C. and Wei, J., "Vibration in a moving flexible robot arm", *J. Soun. Vibr.*, 116, 149-160, 1987.

[25] Yuh, J. and Young, T., "Dynamic modeling of an axially moving beam in rotation: simulation and experiment", *ASME J. Dyna. Sys. Meas. Contr.*, 114, 41-49, 1991.

[26] Stylianou, M. and Tabarrok, B., "Finite element analysis of an axially moving beam, Part I: time integration", *J. Soun. Vibr.*, 178(4), 433-453, 1994.

[27] Stylianou, M. and Tabarrok, B., "Finite element analysis of an axially moving beam, Part II: stability analysis", *J. Soun. Vibr.*, 178(4), 455-481, 1994.

[28] Behdinan, K., *Dynamics of Geometrically Nonlinear Sliding Beams*, Ph. D. Thesis, University of Victoria, 1996.

[29] Behdinan, K., Stylianou, M., and Tabarrok, B., "Dynamics of flexible sliding beams – nonlinear analysis Part I: formulation", *J. Soun. Vibr.*, 208(4), 517-539, 1997.

[30] Behdinan, K. and Tabarrok, B., "Dyanimcs of flexible sliding beams – nonlinear analysis Part II: transient response", *J. Soun. Vibr.*, 208(4), 541-565, 1997.

[31] Kuo, Y.L., *Applications of the h-, p-, r-refinements of the Finite Element Method on Elasto-dynamic Problems*, Ph.D. Thesis, University of Toronto, 2005.

[32] Y.L. Kuo, K. Behdinan, W.L. Cleghorn, and R.G. Fenton, "The *h-p-r*-refinement Finite Element Analysis of an Axially Moving Beam", Proceedings of Canadian Society of Mechanical Engineering Forum, Kananaskis Village, Albert, Canada, May 21-23, 2006.